Stable Free-Standing Lipid Bilayer Membranes in Norland Optical Adhesive 81 Microchannels

Marin, Victor; Kieffer, Roland; Padmos, Raymond; Aubin-Tam, Marie Eve

DOI
10.1021/acs.analchem.6b00926

Publication date
2016

Document Version
Accepted author manuscript

Published in
Analytical Chemistry

Citation (APA)
Marin, V., Kieffer, R., Padmos, R., & Aubin-Tam, M. E. (2016). Stable Free-Standing Lipid Bilayer Membranes in Norland Optical Adhesive 81 Microchannels. *Analytical Chemistry*, *88*(15), 7466-7470. https://doi.org/10.1021/acs.analchem.6b00926

Stable Free-standing Lipid Bilayer Membranes in Norland Optical Adhesive (NOA81) Microchannels

Victor Marin‡, Roland Kieffer‡, Raymond Padmos, and Marie-Eve Aubin-Tam*

Department of Bionanoscience, Kavli Institute of Nanoscience, Delft University of Technology, 2629 HZ, Delft, The Netherlands

KEYWORDS. Lipid bilayer, membrane, microfluidics, surface chemistry, electrophysiology.

ABSTRACT. We report a simple, cost-effective and reproducible method to form free-standing lipid bilayer membranes in microdevices made with Norland Optical Adhesive (NOA81). Surface treatment with either alkylsilane or fluoroalkylsilane enables the self-assembly of stable DPhPC and DOPC/DPPC membranes. Capacitance measurements are used to characterize the lipid bilayer and to follow its formation in real-time. With current recordings, we detect the insertion of single α-Hemolysin pores into the bilayer membrane, demonstrating the possibility of using this device for single-channel electrophysiology sensing applications. Optical transparency of the device and vertical position of the lipid bilayer with respect to the microscope focal plane, allows easy integration with other single-molecule techniques, such as optical tweezers. Therefore, this method to form long-lived lipid bilayers finds a wide range of applications, from sensing measurements to biophysical studies of lipid bilayers and associated proteins.

INTRODUCTION

Artificial lipid bilayers are commonly used to mimic cellular membranes in biophysical studies[1,2], synthetic biology[3,4], drug delivery[5] and diagnostic applications[6]. In particular, free-standing lipid membranes are often required in biophysical applications that necessitate control over the physical and chemical conditions on both sides of the membrane (e.g. electrophysiology). Free-standing lipid bilayers are traditionally formed over small apertures in Teflon thin sheets by "painting" a droplet of lipid dissolved in organic solvent over the orifice[7].

There is an increasing interest in using microfluidic devices, as they offer the benefit of sub-microliter reagents volumes handling, high-sensitive sensing and simple parallelization[8,9]. Although materials like Teflon and glass confer mechanical robustness and long-term stability to the membrane[2,10,11], they lack straightforward cost-efficient micropatterning techniques. Suspended lipid bilayers can be formed over apertures microfabricated in silicon,[12] but this approach prevents combination with optical imaging. Alternatively, polymethilsiloxane (PDMS) is a transparent biocompatible material, which allows low-cost and simple fabrication, but its use for the formation of free-standing lipid bilayers is hindered by swelling and deformability issues in several organic solvents[13], which are often required for artificial lipid bilayer formation[14,15]. Recently, the photopolymer Norland Optical Adhesive 81 (NOA81) has gained attention as a material for fabricating microfluidic systems[16]. NOA81 has been used previously as adhesion layer to glue glass to a film of fluorinated ethylene propylene, where lipid bilayers are formed[17]. Owing to its solvent resistance, optical transparency and easy fabrication, we find NOA81 to be a well-suited material for microfluidic devices hosting lipid bilayers.

Here, we present a novel and straightforward method to fabricate free-standing long-lived lipid membranes in channels entirely made with NOA81 (Fig. 1). A surface treatment with either an alkylsilane or a fluoroalkylsilane enables the self-assembly of stable DPhPC and DOPC/DPPC membranes. Our simple and cost-efficient approach does not require gluing between layers, avoiding alignment and layers attachment, alleviating the risks of leakage and simplifying the fabrication process compared to other reported methods[17-19]. Kinetics of membrane formation is monitored in capacitance measurements. High-resolution current recordings show the insertion of single pores of α-Hemolysin in the membrane.

EXPERIMENTAL

Microfluidic device formation. Microchannels are entirely made of NOA81 (Norland products) sandwiched in between two glass slides (Fig. 1 a,b). Device fabrication follows a straightforward process consisting of three steps:

(1) Fabrication of the PDMS mold. Parallel microchannels connected by a 85 μm-wide aperture are etched on a SU-8 2075 photoresist layer using conventional lithography[20]. A PDMS negative replica is made by curing PDMS onto the SU-8 patterns, gently peeling it off, and subsequently using it as master for NOA81[16]. Due to its flexibility, PDMS is a suitable reusable mold that is easily removed from the NOA81 channels.

(2) Fabrication of the NOA81 device. Liquid NOA81 is poured onto the PDMS replica, and covered with microscope glass slide, which were cleaned with Hellmanex III, rinsed with ethanol, and finally treated with an oxygen plasma at 30% power for 25 s (Plasma Preen I). The

NOA81 layer thickness is controlled with thin metal spacers between the glass slide and the PDMS. NOA81 is cured by a 3-min UV exposition at a wavelength of 365 nm, with 36 W of power (Promed UVL-36 with four UV-9W-L bulbs). The PDMS mold is then removed from the NOA81 microchannels. The channels are washed with ethanol and holes are made for inlets/outlets with a sand blaster. Secondly, a clean glass cover slide is coated with a partially cured NOA81 layer. This is done by spin-coating a thin layer of NOA81 during 5 s at 500 rpm followed by 20 s at 4000 rpm (Spin150i POLOS) and partially curing by UV exposition during 30 s. The partially cured NOA81 layer is gently pressed against the fully cured NOA81, thus closing the channels. To permanently seal the two layers of NOA81, the device is subject to a final UV exposition during 8 min, followed by heating at 50°C during 12 h.

(3) Surface treatment. NOA81 microchannels are cleaned by rinsing the channels with ethanol, followed by flowing nitrogen, and drying at 80°C. To reduce the surface hydrophilicity of the device, the hydroxyl groups present on the NOA81 are functionalized with tri-chloro(1H,1H,2H,2H-perfluorooctyl)silane (PFOTS, Sigma-Aldrich) or with trichloro(octyl)silane (OTS, Sigma-Aldrich). For this silanization treatment, a 1.5 % V/V PFOTS or OTS solution in isooctane is injected inside clean microchannels and incubated for 15 min. After incubation, microchannels are cleaned as before.

Lipid bilayer formation. Lipids – 1,2-diphytanoyl-sn-glycero-3-phoscholine (DPhPC), 1,2-Dioleoyl-sn-glycero-3-phosphocholine (DOPC) and 1,2-dihexadecanoyl-sn-glycero-3-phosphocholine (DPPC) – in chloroform were purchased from Avanti lipids. Chloroform is evaporated with a stream of nitrogen gas during 20 min, followed by incubation in a vacuum

chamber for at least 2 h. Dried lipids were suspended in aqueous buffer (150 mM of KCl, 10 mM of HEPES at pH of 7.4) and stored at 4°C for later use. Microchannels are first filled with organic solvent using a pressure pump (Fluigent MFCS-EZ) pushing at 0.5 mbar in both channels. Afterwards, at the same pressure, we flow a previously sonicated aqueous solution, which contains lipids in 150 mM KCl, 10mM HEPES at pH 7.4.

We form membranes composed of either DPhPC, or of a mixture of DOPC and DPPC in 1:1 molar ratio. For the formation of the DPhPC lipid membrane, the organic solvent is decane, and the aqueous phase contains 3.0 mg/ml DPhPC. For the formation of the DOPC/DPPC lipid membrane, the organic solvent is a mixture of decade/chloroform/methanol at 7:2:1 v/v,[21] and the aqueous phase contains 3.0 mg/ml DOPC and 2.8 mg/ml DPPC. Bilayer membrane formation is observed with bright field microscopy when lipid monolayers enter in contact at the water-solvent interface in the aperture between the channels (Fig. 1a).

To evaluate success rates of lipid bilayer formation under different conditions, a modified microdevice design with a series of multiple rectangular apertures (supporting information) is used. Channels and apertures in this device have the same geometry as in the single gap microdevice.

Sessile drop experiment. For these measurements, glass slides (cleaned as described before) are coated with NOA81, exposed to UV during 10 min and fully cured on a hotplate at 80°C overnight[22]. Half the samples are further treated with either the PFOTS or the OTS silane. Hydrophobicity is characterized by depositing a 7 μl droplet of water (MilliQ, 18.2MΩ.cm at

25°C) on the NOA81 coated slides and the contact angle of the drop is measured[23]. Similarly, lipophilicity is characterized by depositing a 7 µl droplet of decane on the substrate.

Fluorescence confocal microscopy. To image the lipid bilayer in the aperture, 0.15 mg/ml N-(Fluorescein-5-thiocarbonyl)-1,2-dihexadecyl-sn-gycero-3-phosphoethanolamine (Fluor-DHPE, Avanti lipids) is added to the lipid (DPhPC) containing aqueous solution for membrane formation. A Nikon A1R confocal microscope is used for imaging. From the stack of images, a 3D reconstruction is done with ImageJ.

Capacitance measurements. Capacitance was monitored with Ag/AgCl electrodes using triangular signal of 200Hz at 100 mV peak-to-peak with signal generator (BK precision 4040A 20MHZ). A DLPCA 200 (Femto) is used for amplification and current-potential convertor. After a 5KHz low-pass filter, acquisition is done by a DAQ USB-6009 (National Instrument) at a 20KHz rate, and computing is done with homemade LabView script. Membrane conductance and capacitance were calculated considering that the membrane conductance is negligible compared to the conductance of the bulk solution[24,25]. The background capacitance is measured before the formation of the bilayer membrane, and subtracted from the measured total capacitance obtained from the bilayer membrane[26].

Electrophysiology measurements with α-Hemolysin. For the electrophysiology measurements, 3.3 µg/ml of α-Hemolysin (Sigma-Aldrich) is added to the DPhPC aqueous solution, containing

150 mM KCl, 10 mM HEPES at pH 7.4, and flowed in one of the two channels. A Keithley 6517A is used as generator and pico-ampermeter to measure the current flowing through the protein pores present in the bilayer membrane.

RESULTS AND DISCUSSION

We fabricate a microfluidic device consisting of two 100 µm-high and 1 mm-wide parallel channels connected by a 85 µm rectangular aperture where a free-standing lipid bilayer membrane is self-assembled (Fig. 1a). The microchannels are entirely made of NOA81 (Fig. 1b), which prevents swelling and allows easy patterning.

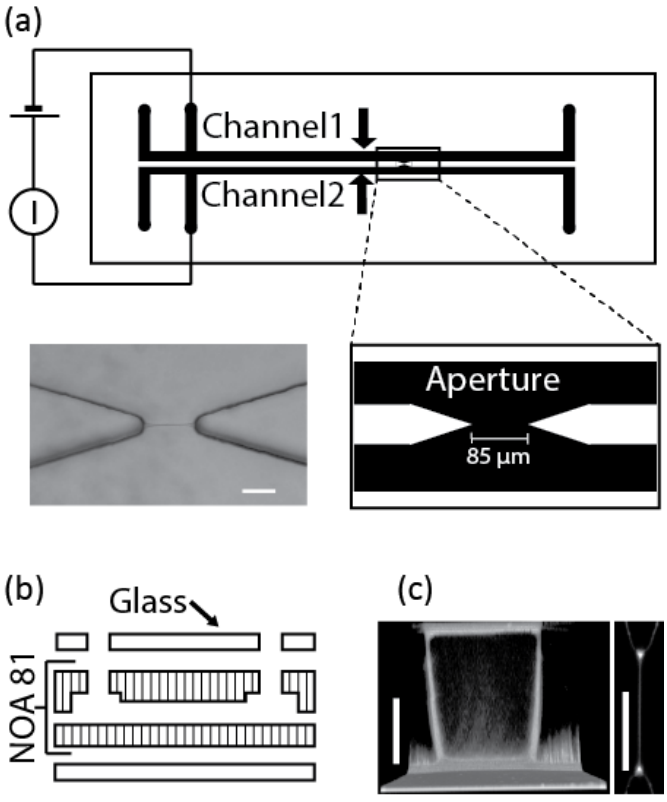

Figure 1. NOA81 microfluidic device used for electrophysiology recording. **a)** Top-view showing microfluidic design: the channels are 100μm high and 1mm wide. The aperture between the channels has a width of 85μm. The top right: picture shows a free-standing lipid membrane in the aperture observed with bright-field. Scale bar: 50 μm. **b)** Cross-section of the NOA81 microfluidic device, which consists of two glass slides sandwiching the NOA81 microchannels. **c)** Front view of the 3D reconstruction (left) and cross-section (right) of a free-standing lipid membrane observed by fluorescence confocal microscopy. Fluorescent lipids (Fluor-DHPE) are used to visualize the lipid membrane and the annulus. At the edge of the lipid membrane, the reservoir (annulus) of lipid molecules shows higher fluorescence intensity than the lipid bilayer membrane. Scale bar: 50 μm.

Characterization of the silanized-NOA81 surface

Prior to lipid membrane formation, a silanization of the surface of the channels is done with either fluoroalkylsilane PFOTS or alkylsilane OTS. The resulting surface properties of silanized NOA81 are characterized by a sessile drop experiment (Table 1). The resulting contact angle values confirm that untreated NOA81 channels are mildly hydrophilic[22,27]. Both surface treatments result in a more hydrophobic surface. With a drop of decane, a contact angle smaller than 10° is found for untreated NOA81 and for OTS-treated NOA81. However, we measured a contact angle of ~70° for PFOTS-treated NOA81. Therefore, the PFOTS treatment increases

both the hydrophobic and lipophobic character of the surface. Surface properties are maintained after one week.

In agreement with these measurements, we observe that the treatment has an impact on the flow in the microchannels. When flowing decane followed by water in untreated NOA81 microchannels, droplets of organic solvent remain attached to the surface (Fig. 2a). In this condition, a pressure of ~10 mbar is required to push the water/decane interface, which prevents membrane formation. With the silane surface treatment, droplets of decane are not seen anymore on the surface (Fig. 2b) and a pressure of 0.5 mbar is sufficient to push the solvent/buffer interface. Under this pressure, lipid bilayer formation in PFOTS- and OTS-treated NOA81 microchannels is reproducible.

Table 1. Contact angle values of water and decane on untreated and silanized NOA81.

		PFOTS-treated NOA81		OTS-treated NOA81	
Contact angle	NOA81	after surface treatment	7 days later	after surface treatment	7 days later
water	69.3°±1.3°	107.8°±1.1°	109.8°±1.3°	99.0°±0.4°	97.7°±1.0°
decane	<10°	68.9°±1.5°	71.0°±1.5°	<10°	<10°

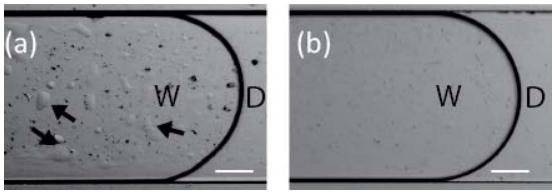

Figure 2. Interface water(W)/decane(D) in a rectangular NOA81 microchannel, without **(a)** and with **(b)** PFOTS treatment, on different devices. Without surface treatment, droplets of decane are observed on the channel surface, as indicated with black arrows. Scale bar is 100 μm.

Formation of free-standing DPhPC and DOPC/DPPC bilayers

Free-standing membranes are formed by subsequently flowing of an organic solvent and an aqueous solution of lipids. The lipid bilayer forms when the two lipid monolayers at the water-solvent interface contact one another in the aperture between the channels. Membrane formation success rate is tested for DPhPC and for a 1:1: mixture of DOPC/DPPC using PFOTS- or OTS-treated multigap flowcells (supporting information). In both PFOTS- and OTS-treated flowcells, DPhPC membranes are formed in ~80% of the apertures. DOPC/DPPC membranes are formed in 66% of apertures of PFOTS-treated channels and 77% of apertures of OTS-treated channels. The majority of such formed free-standing lipid bilayers remain stable for several days.

Fluorescence confocal microscopy is used to measure the surface area of the lipid bilayer and the size of the annulus in the aperture (Fic. 1c). For that purpose, a small amount of fluorescently-labeled DHPE is added to the DPhPC solution. At the edge of the lipid membrane,

we observe a higher fluorescent intensity in the annulus, as it contains a reservoir of lipid molecules[28]. From the stack of images of the membrane and annulus, we estimate that the lipid bilayer has a surface area of 6670 μm^2 (see supporting information for measurement of bilayer surface area).

Electrical measurements of lipid bilayers

Capacitance is monitored to follow the dynamics of bilayer formation of a DPhPC-membrane in a single gap PFOTS-treated flow cells (Fig. 3a). Before the two monolayers enter in contact in the channel aperture, an average background capacitance of C_0 = 6.0 ± 0.2 pF is measured. The measured total capacitance (C_T) reaches a steady state value after ~10 min, when the lipid bilayer reaches its maximum surface area. The average membrane capacitance once the lipid bilayer is fully formed is $C_M = C_T - C_0 = 33 \pm 2$ pF. Since the maximum surface area for the lipid bilayer is the size of the aperture (100 μm X 85 μm), we obtain a specific membrane capacitance of at least 0.4 $\mu F.cm^{-2}$. Considering the lipid bilayer surface area measured with confocal microscopy, we estimate a specific membrane capacitance of ~ 0.5 $\mu F.cm^{-2}$, which is within capacitance values previously reported for DPhPC lipid membranes[29-31], indicating little or no residual decane in the bilayer membrane, and remarkably less than for a bilayer at a droplet interface[30].

The seal resistance for the lipid membrane bilayer formed inside the NOA81 microfluidic device (in absence of proteins) is higher than 10 GΩ[25].

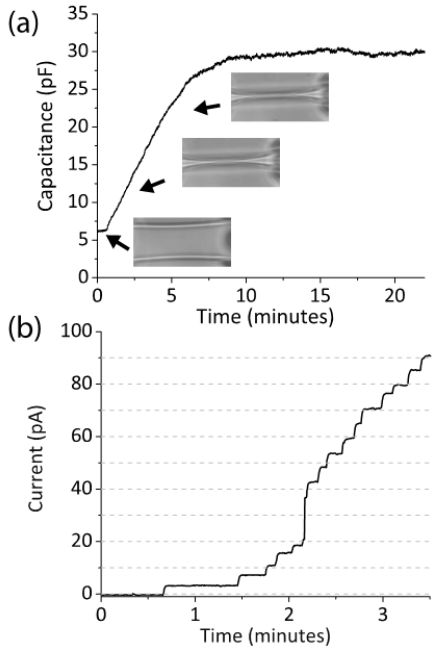

Figure 3. a) The capacitance increases when the lipid bilayer forms and spreads in size, until it reaches its maximum surface area. Pictures of the water/decane interfaces during membrane formation are shown. **b)** High-resolution current recording across the lipid membrane detects single α-Hemolysin pores inserting into the artificial lipid bilayer. Flowing 3.3 µg/ml α-Hemolysin in one channel results in discrete increments in the flux of ions across the lipid bilayer. The current is measured with a picoammeter at 40 mV DC.

Single protein pore insertion

Bilayer formation is also confirmed by inserting α-Hemolysin pores[29,32] into the DPhPC lipid membrane formed in a PFOTS-treated single gap microdevice. Flowing 3.3 μg/ml α-Hemolysin in one of the two channels results in discrete jumps in current (Fig. 3b). With an applied potential of 40 mV, and a buffer containing 150 mM KCl, 10 mM HEPES at pH 7.4, the average single pore current estimated from the electrophysiology recordings is ~5 pA, in agreement with values previously reported for experiments with comparable ionic strength[33]. Under lower pore concentration, this device could be used for single-channel current recording experiments.

CONCLUSIONS

We present a technique to make NOA81 microdevices suitable to form long-lived free-standing lipid bilayers, with easy control over the chemical and physical conditions on both sides of the membrane. For stable lipid bilayer formation, the NOA81 surface is treated with either a fluoroalkylsilane (PFOTS), which reproduces Teflon surface properties, or with an alkylsilane (OTS). Electrophysiology measurements can detect the insertion of single α-Hemolysin protein pores. This highly reproducible method to form stable free-standing lipid bilayers finds a wide range of applications, from drug screening and sensing devices, to biophysical studies of lipid bilayers and membrane protein channels. As the flow cell is optically transparent and the bilayer surface plane is perpendicular to the microscope focal plane, integration with other single-molecule techniques (e.g. optical tweezers) is straightforward, thus enabling combination of real-time electrophysiology recordings with single-molecule force based techniques.

ASSOCIATED CONTENT

Supporting information:

S1: Design of multigap microfluidics device

S2: Measurement of lipid bilayer surface area with fluorescence confocal microscopy

S3: Measurement of lipid bilayer resistance.

AUTHOR INFORMATION

Corresponding Author

*Email: m.e.aubin-tam@tudelft.nl

Author Contributions

‡These authors contributed equally.

Funding Sources

The work was supported by a Marie Curie CIG Grant (618454), and the Netherlands Organization for Scientific Research (VENI NWO Grant 722-013-006).

Notes

The authors declare no competing financial interest.

ACKNOWLEDGMENTS

We thank Andreas Engel for the use of his contact angle measurement device, Jérémie Capoulade for his help with the fluorescence confocal microscopy, and Christophe Danelon for useful discussion.

ABBREVIATIONS

DOPC, 1,2-Dioleoyl-sn-glycero-3-phosphocholine; DPhPC, 1,2-diphytanoyl-sn-glycero-3-phosphocholine; DPPC, 1,2-dihexadecanoyl-sn-glycero-3-phosphocholine; Fluor-DHPE, N-(Fluorescein-5-thiocarbonyl)-1,2-dihexadecyl-sn-gycero-3-phosphoethanolamine; NOA81, Norland optical adhesive 81; OTS, trichloro(octyl)silane; PDMS, polymethilsiloxane; PFOTS, tri-chloro(1H,1H,2H,2H-perfluorooctyl)silane.

REFERENCES

(1) Weatherill, E. E.; Wallace, M. I. *J. Mol. Biol.* **2015**, *427*, 146-157.
(2) Rajapaksha, S. P.; Wang, X.; Lu, H. P. *Anal. Chem.* **2013**, *85*, 8951-8955.
(3) Sachse, R.; Dondapati, S. K.; Fenz, S. F.; Schmidt, T.; Kubick, S. *FEBS Letters* **2014**, *588*, 2774-2781.
(4) Nourian, Z.; Roelofsen, W.; Danelon, C. *Angew. Chem. Int. Edit.* **2012**, *51*, 3114-3118.
(5) Mizuno, M.; Toyota, T.; Konishi, M.; Kageyama, Y.; Yamada, M.; Seki, M. *Langmuir* **2015**, *31*, 2334-2341.
(6) Kukwikila, M.; Howorka, S. *Anal. Chem.* **2015**, *87*, 9149-9154.
(7) Mueller, P.; Rudin, D. O.; Tien, H. T.; Wescott, W. C. *J. Phys. chem.* **1963**, *67*, 534-535.
(8) Zagnoni, M. *Lab Chip* **2012**, *12*, 1026-1039.
(9) Jonsson, P.; Jonsson, M. P.; Hook, F. *Nano Letters* **2010**, *10*, 1900-1906.
(10) Göpfrich, K.; Kulkarni, C. V.; Pambos, O. J.; Keyser, U. F. *Langmuir* **2012**, *29*, 355-364.
(11) Bright, L. K.; Baker, C. A.; Agasid, M. T.; Ma, L.; Aspinwall, C. A. *ACS Appl. Mater. Interfaces* **2013**, *5*, 11918-11926.
(12) Oshima, A.; Hirano-Iwata, A.; Mozumi, H.; Ishinari, Y.; Kimura, Y.; Niwano, M. *Anal. Chem.* **2013**, *85*, 4363-4369.
(13) Dangla, R.; Gallaire, F.; Baroud, C. N. *Lab Chip* **2010**, *10*, 2972-2978.
(14) King, P. H.; Jones, G.; Morgan, H.; de Planque, M. R. R.; Zauner, K.-P. *Lab Chip* **2014**, *14*, 722-729.
(15) Tsuji, Y.; Kawano, R.; Osaki, T.; Kamiya, K.; Miki, N.; Takeuchi, S. *Lab Chip* **2013**, *13*, 1476-1481.
(16) Sollier, E.; Murray, C.; Maoddi, P.; Di Carlo, D. *Lab Chip* **2011**, *11*, 3752-3765.
(17) Bomer, J. G.; Prokofyev, A. V.; van den Berg, A.; Le Gac, S. *Lab Chip* **2014**, *14*, 4461-4464.
(18) Halza, E.; Bro, T. H.; Bilenberg, B.; Kocer, A. *Anal. Chem.* **2013**, *85*, 811-815.
(19) Kendall, E. L.; Shao, C.; DeVoe, D. L. *Small* **2012**, *8*, 3613-3619.
(20) Abgrall, P.; Conedera, V.; Camon, H.; Gue, A.-M.; Nguyen, N.-T. *ELECTROPHORESIS* **2007**, *28*, 4539-4551.
(21) Wodzinska, K.; Blicher, A.; Heimburg, T. *Soft Matter* **2009**, *5*, 3319-3330.
(22) Gu, H.; Duits, M. H. G.; Mugele, F. *Lab Chip* **2010**, *10*, 1550-1556.
(23) Kaufmann, T. C.; Engel, A.; Rémigy, H.-W. *Biophys. J.* **2006**, *90*, 310-317.
(24) Batishchev, O. V.; Indenbom, A. V. *Bioelectrochemistry* **2008**, *74*, 22-25.
(25) Hirano-Iwata, A.; Niwano, M.; Sugawara, M. *TrAC Trends in Analytical Chemistry* **2008**, *27*, 512-520.
(26) Kalsi, S.; Powl, Andrew M.; Wallace, B. A.; Morgan, H.; de Planque, Maurits R. R. *Biophys. J.* **2014**, *106*, 1650-1659.
(27) Wägli, P.; Homsy, A.; de Rooij, N. F. *Sensor. Actuat. B-Chem.* **2011**, *156*, 994-1001.
(28) White, S. H. *Biophys J* **1972**, *12*, 432-445.
(29) Funakoshi, K.; Suzuki, H.; Takeuchi, S. *Anal. Chem.* **2006**, *78*, 8169-8174.
(30) Nikolov, V.; Lin, J.; Merzlyakov, M.; Hristova, K.; Searson, P. C. *Langmuir* **2007**, *23*, 13040-13045.
(31) Gross, L. C. M.; Heron, A. J.; Baca, S. C.; Wallace, M. I. Langmuir **2011**, 27, 14335-14342; Batishchev, O. V.; Indenbom, A. V. *Bioelectrochemistry* **2008**, *74*, 22-25.

(32) Saha, S. C.; Thei, F.; de Planque, M. R. R.; Morgan, H. *Sensor. Actuat. B-Chem.* **2014**, *199*, 76-82.
(33) Suzuki, H.; Tabata, K. V.; Noji, H.; Takeuchi, S. *Biosens. Bioelectron.* **2007**, *22*, 1111-1115.